In Vitro Proliferation of Cells Derived From Adult Human β-Cells Revealed By Cell-Lineage Tracing

Holger A. Russ,[1] Yael Bar,[1] Philippe Ravassard,[2] and Shimon Efrat[1]

OBJECTIVE—Expansion of insulin-producing β-cells from adult human islets could alleviate donor shortage for cell-replacement therapy of diabetes. A major obstacle to development of effective expansion protocols is the rapid loss of β-cell markers in the cultured cells. Here, we report a genetic cell-lineage tracing approach for following the fate of cultured β-cells.

RESEARCH DESIGN AND METHODS—Cells dissociated from isolated human islets were infected with two lentiviruses, one expressing Cre recombinase under control of the insulin promoter and the other, a reporter cassette with the structure cytomegalovirus promoter-loxP-DsRed2-loxP-eGFP.

RESULTS—β-Cells were efficiently and specifically labeled by the dual virus system. Label$^+$, insulin$^-$ cells derived from β-cells were shown to proliferate for a maximum of 16 population doublings, with an approximate doubling time of 7 days. Isolated labeled cells could be expanded in the absence of other pancreas cell types if provided with medium conditioned by pancreatic non–β-cells. Analysis of mouse islet cells by the same method revealed a much lower proliferation of labeled cells under similar culture conditions.

CONCLUSIONS—Our findings provide direct evidence for survival and dedifferentiation of cultured adult human β-cells and demonstrate that the dedifferentiated cells significantly proliferate in vitro. The findings confirm the difference between mouse and human β-cell proliferation under our culture conditions. These findings demonstrate the feasibility of cell-specific labeling of cultured primary human cells using a genetic recombination approach that was previously restricted to transgenic animals. *Diabetes* 57:1575–1583, 2008

R estoration of an adequate β-cell mass is the central therapeutic goal in patients with type 1 diabetes. However, pancreatic islet transplantation is severely limited by the number of organ donors. Studies of adult islet renewal in vivo suggest that

From the [1]Department of Human Molecular Genetics and Biochemistry, Sackler School of Medicine, Tel Aviv University, Ramat Aviv, Tel Aviv, Israel; and [2]Unité Mixte de Recherche 7091, National Center for Scientific Research, Hôpital Pitié Salpêtrière, Pierre and Marie Curie University, Paris, France.

Corresponding author: Shimon Efrat, Department of Human Molecular Genetics and Biochemistry, Sackler School of Medicine, Tel Aviv University, Ramat Aviv, 69978 Tel Aviv, Israel. E-mail: sefrat@post.tau.ac.il.

CMV, cytomegalovirus; eGFP, enhanced green fluorescent protein; EMT, epithelial-to-mesenchymal transition; MOI, multiplicity of infection; MSC, mesenchymal stem cell; NP40, Nonidet P-40; PARP, poly(ADP-ribose) polymerase; RIP-Cre, pTrip RIP405 nlsCRE DeltaU3.

differentiated β-cells maintain a replication capacity (1). However, success in expansion of functional insulin-producing β-cells in vitro has been limited. Culture of adult human islets resulted in a small number of cell population doublings and loss of insulin expression (2–5). Insulin$^-$ cells derived from such cultures could be induced to re-express insulin; however, insulin levels were low and varied considerably among cells from different donors (6–8). In the absence of stable markers for cultured β-cells, it was not possible to determine whether the loss of β-cell phenotype in the expanded cells reflected β-cell dedifferentiation or β-cell death accompanied by expansion of islet cells from a non–β-cell origin. Efficient expansion of dedifferentiated human β-cells in vitro could be of therapeutic significance because these cells may retain enough of their specific open chromatin structure to facilitate their redifferentiation. Genetic cell-lineage tracing provided evidence for dedifferentiation of cultured mouse β-cells (9); however, it could not detect a significant proliferation of the dedifferentiated cells (9–12). Rather, under the culture conditions used, these cells were eventually eliminated, giving rise to cultures dominated by cells derived from non–β-cells. Here, we applied a genetic cell-lineage tracing approach for following the fate of cultured adult human β-cells using viral vector-mediated gene transfer. Our findings demonstrate that, in contrast to mouse β-cells, dedifferentiated human β-cells can be significantly expanded in culture.

RESEARCH DESIGN AND METHODS

Lentivirus vector construction and virus production. The pTrip RIP405 nlsCRE DeltaU3 (RIP-Cre) vector was generated by removing with *Bam*HI and *Xho*I of the enhanced green fluorescent protein (eGFP) coding region from the pTrip RIP405 eGFP DeltaU3 vector (13), which contains a fragment of the rat insulin II gene from −405 to +7 relative to the transcription start site. The resulting linearized plasmid was blunt-ended with DNA polymerase I Klenow fragment. The reading frame A Gateway cassette (Gateway Conversion kit; Invitrogen) was next ligated to the blunt-ended vector according to the manufacturer's instructions, generating a pTrip RIP405 rfa-Gateway DeltaU3 destination vector. The nlsCRE fragment was amplified by PCR from a plasmid (14) provided by Guilan Vodjdani (Hôpital de la Pitié, Salpêtrière, Paris) using the forward primer 5′-CACCAGATCTATGCCCAAGAAGAAG AGG-3′ and the reverse primer 5′-CTCGAGCTAATCGCCATCTTC-3′, and the resulting PCR product was cloned into the pENTR/D/TOPO plasmid (Invitrogen) to generate an nls-CRE entry clone. Both destination vector and entry clone were used for in vitro recombination using the LR clonase II system (Invitrogen) according to the manufacturer's instructions. The reporter vector was constructed by amplifying the loxP-DsRed2-loxP cassette by PCR from a plasmid provided by Isabelle Houbracken (Free University, Brussles, Belgium) using the forward primer 5′-AATTCACTAGTGAACCTCTTC-3′ and the reverse primer 5′-GATCCGATCATATTCAATAA-3′. The resulting PCR product was ligated into the blunt-ended *Bam*HI site of the pTrip cytomegalovirus (CMV) eGFP DeltaU3 vector (13), resulting in the pTrip CMV-loxP-DsRed2-loxP-eGFP DeltaU3 lentiviral vector. Virus particles were produced in 293T cells after vector cotransfection with the pCMVdR8.91 and pMD2.G plasmids. The culture medium was harvested 36–48 h later.

Islet cell culture and infection with viruses. Human islets of Langerhans were provided by the Cell Isolation and Transplantation Center at the University of Geneva School of Medicine (Geneva) and San Raffaele Hospital (Milan, Italy) through the European Consortium for Islet Transplantation

"Islets for Research" distribution program sponsored by the Juvenile Diabetes Research Foundation and by the Diabetes Cell Therapy Unit, Faculty of Medicine, Lille 2 University (Lille, France). Islet purity was determined by staining with dithizone. Islets were received 2–3 days after isolation. Islets from individual donors were dissociated into single cells and cultured in CMRL 1066 medium containing 5.6 mmol/l glucose and supplemented with 10% fetal bovine serum, 100 units/ml penicillin, 100 μg/ml streptomycin, 100 μg/ml gentamicin, and 5 μg/ml amphotericine B as described previously (6). After 1–2 days in culture, cells were washed with PBS and infected with a 1:1 mixture of the two viruses at multiplicity of infection (MOI) 3:1 in CMRL containing 8 μg/ml polybrene overnight. βTC-tet cells were infected at MOI 1.5:1. The medium was then replaced with regular culture medium. Cells were re-fed twice a week and split 1:2 once a week. Cell mortality rate was determined in six-well plates by collecting floating cells 24-h after plating and staining with trypan blue. The adherent cells were trypsinized and similarly stained. Conditioned medium was obtained 2–3 days after the last change of medium, centrifuged at 1,000 rpm for 4 min, filtered with a 0.22-μm filter, and stored at −20°C. Mouse islets were isolated from 5-month-old BALB/c mice by collagenase infusion through the bile duct and treated similarly to the human islets.

Cell sorting. Labeled cells were sorted using a fluorescence-activated cell sorter (FACS) (Aria cell sorter; Becton Dickinson, San Jose, CA) with a fluorescein isothiocyanate filter (530/30 nm) for eGFP and a Pe-Texas Red filter (610/20 nm) for DsRed2. Dead cells stained with 7-amino actinomycin D (Invitrogen) were excluded using a PerCP-Cy5.5 filter (695/40 nm). Islet cells infected with the reporter virus alone or with the Turbo GFP virus (Sigma) were used for setting the gating for DsRed2 and eGFP, respectively.

Immunofluorescence. Cells seeded on sterilized coverslips were washed with PBS and fixed with 4% paraformaldehyde for 10 min at room temperature. For nuclear antigens, slides were permeabilized for 10 min with 0.25% Nonidet P-40 (NP40). Cells were blocked for 20 min with 5% fetal goat serum, 1% bovine serum albumin, and 0.2% saponin and incubated for 1 h with the primary antibodies diluted in blocking solution. Cells were then washed and incubated for 40 min with the secondary antibodies. Images were taken using a Zeiss LTM 200 Apotome. Images of fluorescent living cells were taken with a long-distance objective on a Zeiss LTM 200 microscope. Expression of eGFP was detected using mouse anti-GFP (1:500; Chemicon) or rabbit anti-GFP (1:1,000; Invitrogen). DsRed2 was visualized by endogenous fluorescence. Other primary antibodies used are as follows: mouse anti-insulin (1:1,000; Sigma), guinea pig anti-insulin (1:1,000; Dako), mouse anti-human C-peptide (1:200; Biodesign), rabbit anti-human C-peptide (1:100; Abcam), mouse anti-glucagon (1:2,000; Sigma), rabbit anti-somatostatin (1:200; Dako), rabbit anti-pancreatic polypeptide (1:200; Dako), rabbit anti-amylase (1:200; Sigma), mouse anti-cytokeratin 19 (1:50; Sigma), mouse anti-Cre (1:2,000; Chemicon), rabbit anti-Cre (1:1,000; Novagen), rabbit anti-human Ki67 (1:50; Zymed), rabbit anti-mouse Ki67 (1:100; Neo markers), and mouse anti-vimentin (1:50; Calbiochem). Secondary antibodies used are as follows: anti-mouse, anti-rabbit, or anti–guinea pig AMCA (1:200; Jackson), Cy2 (1:200; Biomed), Cy3 (1:300; Biomed), and Alexa 700 (1:100; Invitrogen). DNA was stained with DAPI (Sigma).

DNA analysis. Cell genomic DNA was isolated using the High Pure PCR template preparation kit (Roche Molecular Biochemicals, Mannheim, Germany). PCR analysis of the integrated reporter vector was performed with the forward primer 5′-AACAACTCCGCCCCATTG-3′ and the reverse primer 5′-CTCCTCGCCCTTGCTCAC-3′. This primer pair amplifies a 1,129-bp fragment from the original sequence and a 338-bp fragment from the recombined sequence. PCR products were resolved on a 1.5% agarose gel containing ethidium bromide.

RNA analysis. Total RNA was extracted using the High Pure RNA isolation kit (Roche Molecular Biochemicals). Total RNA was amplified using the Ovation Aminoallyl RNA Amplification and Labeling System (Nugen). cDNA quantitation was performed using the following Assay-on-Demand kits (Applied Biosystems): insulin, Hs_00355773_m1; *PDX1*, Hs_00426216_m1; *NKX2.2*, Hs_00159616_m1; glucagon, Hs_00174967_m1; *NEUROD1*, Hs_00159598_m1; *NKX6.1*, Hs_00232355_m1; glucokinase, Hs_00175951_m1; PC1/3, Hs00175619_m1; PC2, Hs_00159922_m1; GLUT2, Hs_01096908_m1; *PTF1a*, Hs_00603586_g1; *HNF4a*, Hs_00230853_m1; *PAX4*, Hs_00173014_m1; *PAX6*, Hs_00240871_m1; *HNF6*, Hs00413554_m1; *NGN3*, Hs00360700_g1; vimentin, Hs00185584_m1; and RPLP0, Hs_99999902_m1. All reactions were done in triplicate. The results were normalized to human large ribosomal protein P0 cDNA (RPLP0).

Immunoblotting. Total protein was extracted by incubating cells for 10 min in 1% NP40 containing a protease inhibitor cocktail. Protein concentration was determined using the BCA Protein Assay kit (Pierce). Forty micrograms of protein were resolved on an SDS-PAGE gel. The gel was electroblotted onto Immobilon-P Transfer Membrane (Millipore), followed by incubation with rabbit anti-cleaved poly(ADP-ribose) polymerase (PARP) (1:1,000; Cell Signaling) or rabbit anti-p21 (1:200; Santa Cruz). Goat anti-actin (1:1,000; Santa Cruz)
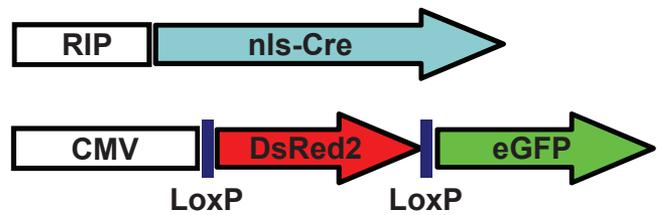

FIG. 1. Schematic representation of the two lentivirus vectors. nls, nuclear localization signal.

was used to monitor gel loading. The bound antibody was visualized with the appropriate horseradish peroxidase–conjugated anti-IgG and SuperSignal West Pico Chemiluminescent Substrate (Pierce). Cells treated with 1 μmol/l staurosporine for 6 h were used as positive control.

Statistical analysis. Significance was determined using a two-tailed Student's *t* test.

RESULTS

The labeling approach is based on cell infection with a mixture of two lentivirus vectors, one expressing Cre recombinase under control of the insulin promoter (RIP-Cre) and the other, a reporter cassette with the structure CMV promoter-loxP-DsRed2-loxP-eGFP (Fig. 1). The latter virus expresses the fluorescent marker DsRed2 in all cells infected by it, while expression of eGFP is blocked. Removal of the DsRed2 coding sequence between the two loxP sites in β-cells infected by both viruses is expected to eliminate DsRed2 expression specifically in these cells and activate instead eGFP expression, which should allow continuous tracking of β-cell fate after insulin expression is lost. Human β-cells were shown to maintain insulin expression during the initial days in culture (6), thereby providing a window of time for RIP-Cre expression. Non–β-cells infected with both viruses are expected to express only DsRed2.

The specificity of the labeling system was evaluated using the mouse β-cell line βTC-tet and 293T cells as a negative control. No eGFP$^+$ cells were detected in 293T cells infected with the reporter virus alone or with a mixture of the two viruses (Fig. 2), demonstrating a tight inhibition of eGFP expression in the absence of RIP-Cre expression. This finding demonstrates the lack of nonspecific RIP-Cre expression, such as could potentially be caused by virus integration next to a strong promoter, and a lack of GFP expression in the presence of the DsRed2 region. In contrast, Cre expression under CMV promoter resulted in efficient activation of eGFP expression. Presence of both eGFP and DsRed2 proteins in the same cells, manifested by yellow color, likely reflects the relatively long half-life of the DsRed2 protein (4.5 days), which may still be detected 1–2 weeks after loss of the DsRed2 gene and activation of eGFP expression. In βTC-tet cells infected with the reporter virus alone, 61.2% of the cells became DsRed2$^+$, indicating a high efficiency of cell infection with this vector (based on >1,000 cells counted in micrograph images; Fig. 3A). In cells infected with the RIP-Cre virus alone, 100% of Cre$^+$ cells were also insulin$^+$ (Fig. 3B). Given the infection efficiency with a single virus, in cells infected with both viruses, the incidence of eGFP$^+$ and DsRed2$^+$ cells is expected to be 37.4% (0.612 × 0.612) and 23.8% (0.612–0.374), respectively. The observed incidence was 32.3 and 30.6% for eGFP$^+$ and DsRed2$^+$, respectively (based on >1,000 cells counted in micrograph images; Fig. 3A). All eGFP$^+$ cells (100%) stained for insulin (Fig. 3C).
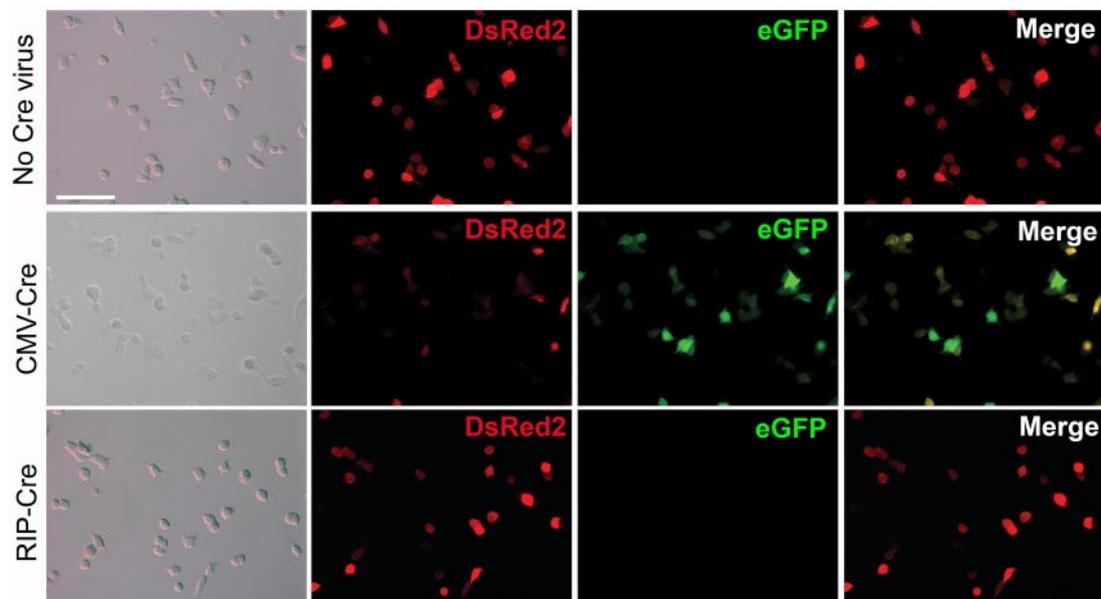
FIG. 2. Assay of the two-virus system in 293T cells. Cells were infected with the reporter virus alone or in combination with a CMV-Cre or a RIP-Cre virus. Live cells were photographed 4 days after infection for DsRed2 (*red*) and eGFP (*green*) autofluorescence. All cells were visualized using a Nomarsky lens (*left*). Bar = 100 μm.

Islets were isolated from 15 human donors, 10 males and 5 females, aged 17–60 years (mean age 46 ± 12 years), with a purity ranging between 70 and 90% (mean 78 ± 6%), as determined by staining with dithizone (Supplementary Table 1, available in an online appendix at http://dx.doi.org/10.2337/db07-1283). Islets from each donor were dissociated into single cells and cultured as described previously (6). Because human islets were reported to contain on average 55% insulin$^+$ cells (15), these preparations were expected to contain <43 ± 3% insulin$^+$ cells at the time of isolation (0.55 × 0.78). After 1–2 days in culture, the cells were infected with the reporter virus alone or with a mixture of the two viruses. At the time of infection, the number of insulin-expressing cells was expected to be lower compared with their number immediately after isolation because of rapid dedifferentiation during the 2–3 days of shipment and 1–2 days of initial culture (6). Cells infected with the reporter virus alone showed DsRed2 expression in 68.2 ± 11.0% of the cells (based on flow cytometry analysis of cells at passages 2–6, derived from five donors, 2–10 × 10^3 cells per sample; Fig. 4*A*), demonstrating a high efficiency of cell infection with this vector. An eGFP signal was shown in <0.08% of the cells, indicating a low leakiness of eGFP expression in these cells in the absence of Cre expression. In islet cells infected with both viruses, 17.9 ± 6.8% of the cells were labeled with eGFP, whereas 41.5 ± 7.4% of the cells were DsRed2$^+$ (based on flow cytometry analysis of cells at passages 2–5, derived from five donors, 2–10 × 10^3 cells per sample, ranging between 8.7 and 31.5% eGFP$^+$ cells; Fig. 4*A*). The calculated labeling efficiency, based on the efficiency of infection with a single virus (68.2%) and the expected β-cell content (<43 ± 3%) given the islet purity, was 20% (0.682 × 0.682 × 0.43). The observed incidence of eGFP$^+$ cells, 17.9 ± 6.8%, is not far from this value. Similarly, the calculated labeling efficiency for DsRed2$^+$ cells was 48.2% (68.2–20%), whereas the observed value was 41.5 ± 7.4%. The ~40% unlabeled cells likely include uninfected cells and cells infected by the RIP-Cre virus alone, whereas the DsRed2$^+$ cells represent non–β-cells

infected by the reporter virus alone or both viruses and β-cells infected by the reporter virus alone.

Among eGFP$^+$ cells, 65.5 ± 7.1% were insulin$^+$, and 68.9 ± 8.9% were human C-peptide$^+$, as judged by immunostaining after 5–6 days in culture (Fig. 5*A*). This was the earliest time point (4–5 days after infection) at which eGFP could be clearly detected in live cells. A weak eGFP signal was detected earlier than 4–5 days after infection. However, it took a longer time for a strong signal to appear, probably due to accumulation of higher levels of eGFP in the cells. We waited for a strong, unequivocal, signal to appear before scoring the cells. To exclude insulin uptake, costaining for insulin and C-peptide was performed; 99.3 ± 0.4% of the insulin$^+$ cells stained for C-peptide (based on counting 1,000 cells from each of three donors after 5 days in culture), indicating that they were bona fide insulin-producing cells (Supplementary Fig. 1). The insulin$^-$ eGFP$^+$ cells likely reflect a rapid loss of insulin content between the time of gene recombination and immunostaining (Fig. 5*A*, *inset*). To further verify this possibility, cells were incubated after viral infection with 10 μmol/l diazoxide, an inhibitor of insulin release (16). This treatment resulted in an increase in the fraction of eGFP$^+$ cells that were insulin$^+$ to 84.8 ± 5.8% (Fig. 5*A*). It is possible that a higher concordance between insulin and eGFP could have been achieved by performing the labeling in the presence of lower glucose concentrations. However, we aimed at performing the labeling at 5.6 mmol/l glucose, a concentration that was optimized for cell proliferation. The rate of insulin content loss at this concentration was expected to be moderate. Because Cre expression could be detected in the cells at an earlier time point after viral infection, compared with eGFP, the concordance between Cre and insulin expression was analyzed 36 h after infection. The analysis revealed that 96.2 ± 0.6% of the Cre$^+$ cells were insulin$^+$ (based on >1,000 cells counted from each of three donors). The concordance between Cre and C-peptide expression analyzed 21 h after infection was even higher, with 98.2 ± 0.6% of the Cre$^+$ cells staining for C-peptide (Fig. 4*B*). The efficiency of β-cell labeling, as
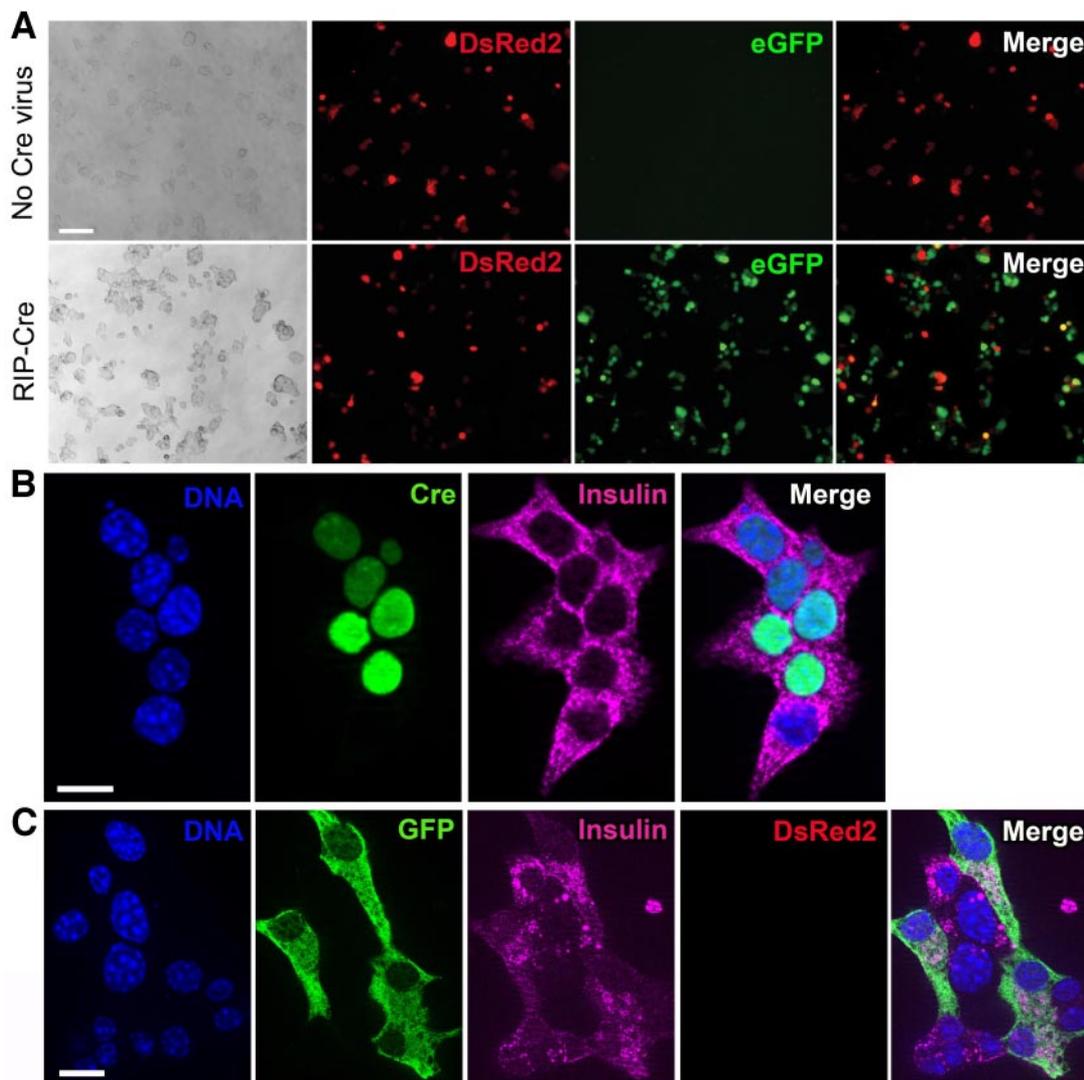
FIG. 3. Labeling of βTC-tet cells with the two-virus system. *A*: Visualization of live cells. βTC-tet cells were infected with the reporter virus alone or in combination with a RIP-Cre virus. Live cells were photographed 4 days after infection for DsRed2 (red) and eGFP (green) autofluorescence. All cells were visualized with phase contrast (*left*). Bar = 100 μm. *B*: Immunofluorescence analysis of βTC-tet cells infected with the RIP-Cre virus. Nuclei are stained blue with DAPI. Bar = 10 μm. *C*: Immunostaining of βTC-tet cells infected with both viruses for insulin and eGFP. DsRed2$^+$ cells are not seen in this field. Bar = 10 μm.

judged by the percentage of C-peptide$^+$ cells labeled with eGFP 4–5 days after infection, was 57.5 ± 8.9% (Fig. 5*A*).

To evaluate the incidence of nonspecific labeling of other pancreatic cells, the infected cells were stained with antibodies for three other islet hormones; for amylase, a marker of pancreatic exocrine cells; and for CK19, a marker of pancreatic duct cells. Of the eGFP$^+$ cells, 11.3 ± 7.6% were stained for glucagon, accounting for 13.7 ± 4.7% of glucagon$^+$ cells (Fig. 5*A*). Of the eGFP$^+$ cells, 1.0 ± 0.6% were stained for somatostatin, whereas 1.2 ± 0.3% were pancreatic polypeptide$^+$, accounting for 5.0 ± 1.8 and 4.7 ± 2.1% of the cells staining for each hormone, respectively. Human islets were reported to contain on average 38% glucagon$^+$ and 10% somatostatin$^+$ cells, respectively (15). Costaining with insulin showed that a large part of eGFP$^+$ cells expressing other islet hormones coexpressed insulin, indicating that their labeling by eGFP was specific, whereas the remainder may have expressed insulin at the time of viral infection but had lost its expression during the time between infection and staining. Coexpression of islet hormones has been documented in human fetal islets

(17,18) but not in adult islets. Its appearance in some cultured adult islet cells (Fig. 5*C*) may represent a stage in cell dedifferentiation in which the cells regress to a fetal-like phenotype. As shown in Fig. 5*A*, <0.1% of amylase$^+$ or CK19$^+$ cells were stained with eGFP. Thus, the bulk of insulin$^-$ eGFP$^+$ cells did not stain for any of the other markers analyzed. All cells stained for the mesenchymal marker vimentin (data not shown), which was shown to be activated in all cultured islet cells (6). Infection of cells at passages 7–8, at which no insulin$^+$ cells could be detected, with both viruses did not result in cell labeling with eGFP, providing further evidence for the dependence of transgene recombination on insulin expression (data not shown). Taken together, these findings demonstrate that the labeling of β-cells with eGFP in this system was efficient and specific.

The eGFP$^+$ cells were followed in the mixed cell population during continuous culture. As previously reported (6), the cultured islet cells replicated with an average doubling time of 7 days, as judged by cell counting, for up to 16 population doublings, before undergoing
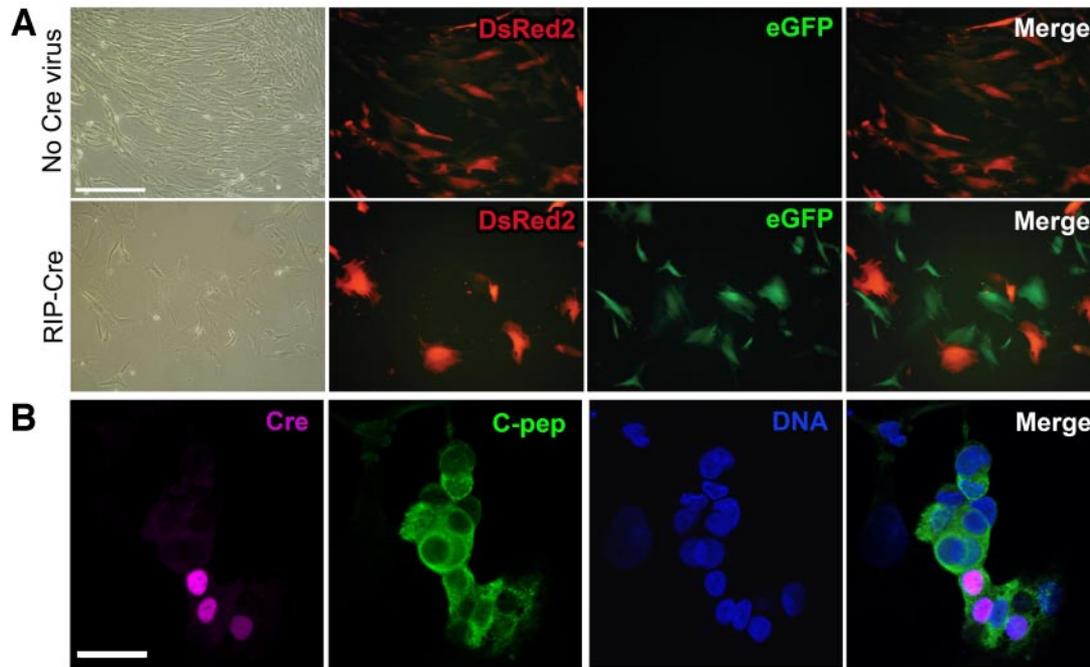
FIG. 4. Labeling of human islet cells with the two-virus system. *A*: Dissociated islet cells were infected with the reporter virus alone or in combination with a RIP-Cre virus. Live cells were photographed at passage 7 for DsRed2 (red) and eGFP (green) autofluorescence. All cells were visualized with phase contrast (*left*). Bar = 100 μm. *B*: Islet cells infected with the RIP-Cre virus alone were stained 21 h after infection with Cre and C-peptide antibodies. Nuclei were stained blue with DAPI. Bar = 20 μm.

senescence. Cell mortality rate, documented in cells from three donors during the first seven passages in culture, averaged 3.5% ($1.0 \pm 0.8\%$ of adherent cells were trypan blue[+], and in addition, $2.5 \pm 1.9\%$ of plated cells were nonadherent and trypan blue[+] 24 h after plating). Thus, the plating efficiency was high, and most cells survived in culture. As seen in Fig. 6*A*, replicating eGFP^{+} cells could be detected during the entire expansion period, as manifested by staining for Ki67 at passages 2, 4, 6, 12, and 14. At passage 2, $31.1 \pm 5.0\%$ of eGFP^{+} cells stained for Ki67. The proportion of eGFP^{+} cells among cultured cells remained stable during this expansion period (Fig. 6*B*), demonstrat-
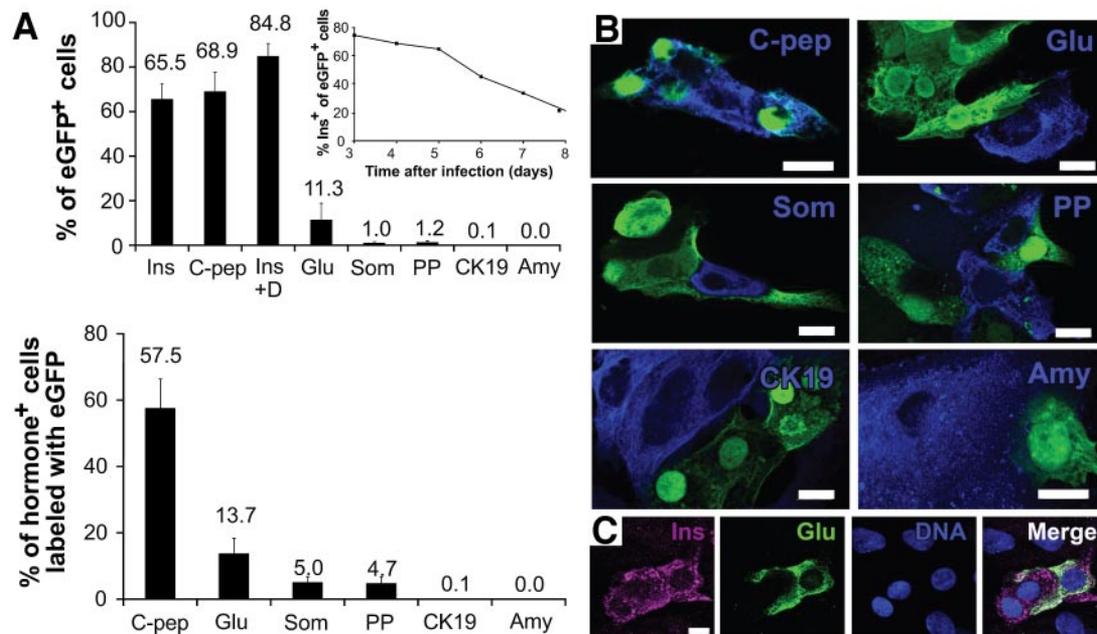

FIG. 5. Specificity of β-cell labeling in the mixed islet cell population. *A*: The fraction of eGFP^{+} cells expressing individual islet hormones, CK19, or amylase on days 5–6 of the culture (4–5 days after viral infection) (*top*) and the fraction of cells positive for each protein that were labeled with eGFP (*bottom*). +D, cells incubated with diazoxide. Data are means ± SD ($n = 3$), based on >1,000 cells counted for each protein from each of three donors. The *inset* on *top* shows data from a representative donor, based on >500 cells counted at each time point. Note that the data for the three non–β-cell hormones includes cells that were double-positive for insulin and the respective hormone; the latter are therefore also included in the fraction of eGFP[+]/ins^{+} cells. *B*: Representative cells from the experiment in *A* immunostained for the indicated pancreatic proteins (blue) and eGFP (green). eGFP is detected in both cytoplasm and nucleus. Bar = 10 μm. *C*: Costaining for glucagon and insulin in cells cultured for 5 days. Nuclei were stained blue with DAPI. Bar = 10 μm.
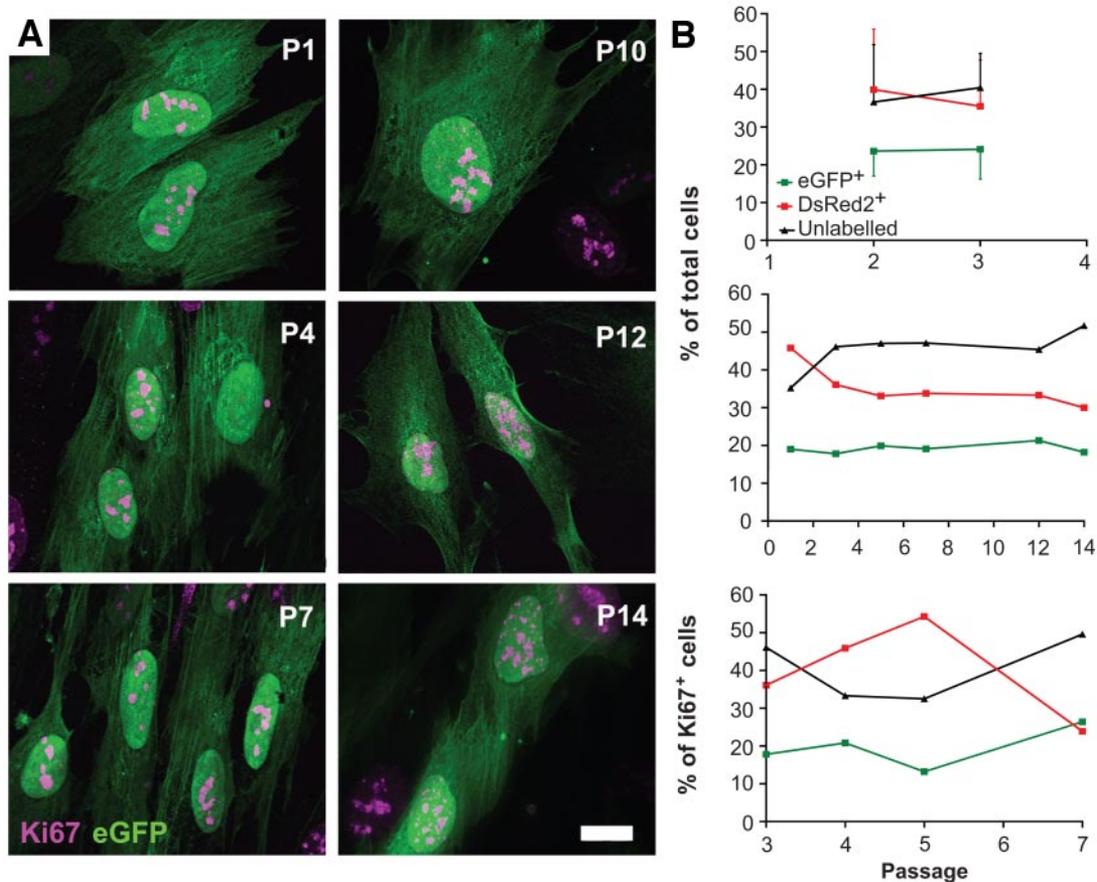
FIG. 6. Replication of eGFP⁺ cells in mixed islet cell culture. *A*: Immunostaining for Ki67 (magenta) and eGFP (green) in cells analyzed at the indicated passages. Bar = 10 μm. *B*: *Top*, incidence of eGFP⁺, DsRed2⁺, and unlabeled cells among all cells at the indicated passages based on cell cytometry of 2–10×10³ cells in each sample. Data are means ± SD (*n* = 4 donors). *Middle* and *bottom*, incidence of each cell type among all cells (*middle*) and among Ki67⁺ cells (*bottom*) in consecutive passages of cultured islet cells from a representative donor based on >1,000 cells counted at each passage.

ing that the doubling rate of the eGFP⁺ cells was similar to that of the eGFP⁻ cells. Overall, replicating eGFP⁺ cells were detected in multiple passages of islet cell cultures from 15 of 15 adult donors studied. The data were highly reproducible among all donors studied, and no age- or sex-related differences were noted. Taken together, these findings demonstrate that dedifferentiated β-cells survive and replicate for a considerable number of population doublings and can be traced during this period by following the eGFP label.

These findings are in contrast to the inability to demonstrate continuous in vitro proliferation of mouse β-cells labeled by transgenic approaches. We therefore used the viral labeling strategy to evaluate mouse β-cell proliferation under conditions similar to those used for human cells. Isolated mouse islets were trypsinized and infected with the two lentiviruses. The efficiency of mouse β-cell labeling (Supplementary Fig. 2) was lower than that of human β-cells: 22.3 ± 0.5%, compared with 57.5 ± 8.9 in human cells (based on counting 500 mouse cells 10 days after infection in each of four independent experiments). At that time point, 3.3 ± 1.8% of mouse eGFP⁺ cells were Ki67⁺, compared with 31.0 ± 5.0% of human eGFP⁺ cells (*P* = 1.7E-06; based on counting 500 mouse cells in each of four independent experiments; Supplementary Fig. 2). Ki67⁺ cells were 10-fold more frequent among mouse eGFP⁻ compared with mouse eGFP⁺ cells. By day 20 after infection, 14 of 1,017 mouse cells counted (1.37%) were

eGFP⁺, which is close to the incidence of 0.55% observed in the transgenic mouse islet cell cultures at that time point (9). In contrast, the human islet cell culture at this time point consisted of 24.1 ± 7.9% eGFP⁺ cells (Fig. 6*B*). These findings confirm the species difference between mouse and human β-cell proliferation under our culture conditions.

eGFP⁺ and DsRed2⁺ cells from the human islet cultures were sorted by FACS and analyzed for transgene recombination and gene expression (Fig. 7*A*). DNA analysis of the sorted cells detected the recombined gene only in eGFP⁺ cells, whereas DsRed2⁺ cells contained only the original gene (Fig. 7*B*). Quantitative RT-PCR analysis of RNA extracted from eGFP⁺ and DsRed2⁺ cells at passages 2 and 12 documented the enrichment of β-cell markers in eGFP⁺ compared with DsRed2⁺ cells at passage 2 and the dedifferentiation of eGFP⁺ cells by passage 12 (Table 1). However, transcript levels in eGFP⁺ cells at passage 2 were 5- to 37-fold lower, compared with the unsorted islet cell population at passage 0. Glucagon transcripts were detectable in eGFP⁺ cells, confirming the immunofluorescence results (Fig. 5); however, they were enriched in DsRed2⁺ cells. Low levels of insulin, PC2, glucagon, and *PAX6* transcripts were still detectable in eGFP⁺ cells at passage 12; however, all other β-cell transcripts were not detected at this stage. Transcripts for *PTF1a*, *HNF6*, and *NGN3*, which are expressed during
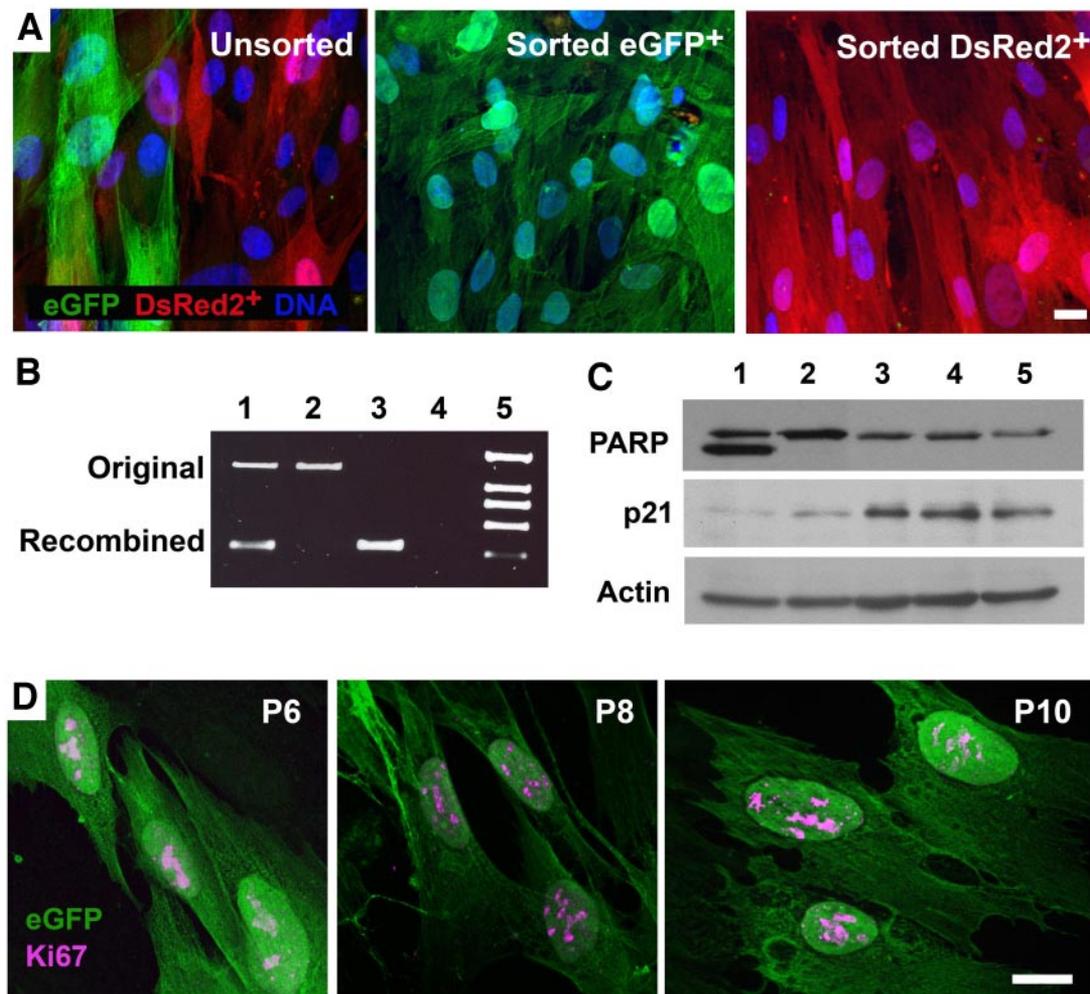
FIG. 7. Analyses of FACS-sorted eGFP⁺ cells. *A*: Mixed cell population at passage 12 (*left*) and eGFP⁺ (*middle*) and DsRed2⁺ (*right*) cells sorted at passage 8 and visualized by eGFP immunofluorescence (green) and DsRed2 self-fluorescence (red). Nuclei are stained blue with DAPI. All panels are merged from micrographs of the three individual colors. Bar = 20 μm. *B*: PCR analysis of DNA from unsorted cells at passage 8 (*lane 1*) and DsRed2⁺ (*lane 2*) and eGFP⁺ (*lane 3*) cells sorted at the same passage, with primers for the reporter vector. *lane 4*, uninfected cells. *lane 5*, DNA ladder. The analysis was reproducible in cells from three donors, of which one is shown. *C*: Immunoblotting of protein from replicating cells at passage 10 with (*lane 1*) or without (*lane 2*) treatment with the apoptotic agent staurosporin, and from unsorted (*lane 3*), and DsRed2⁺ (*lane 4*) and eGFP⁺ (*lane 5*) cells sorted at passage 8, and analyzed at passage 16 with the indicated antibodies. *D*: Immunostaining for Ki67 (magenta) and eGFP (green) in eGFP⁺ cells sorted at passage 5, propagated thereafter in the presence of conditioned medium, and analyzed at the indicated passages. Bar = 10 μm.

pancreas development, were not detected in any of the samples.

We next analyzed the replication capacity of sorted eGFP⁺ cells. Compared with a doubling time of 7 days in the mixed population, eGFP⁺ cells sorted at passage 8 with a purity >90% grew very slowly and doubled approximately once in 4 weeks. Supplementing the culture medium with 50% medium conditioned for 2 days by the mixed islet cell population at passage 0 or for 3 days by passage 10 DsRed2⁺ cells sorted at passage 8 resulted in a decrease in the doubling time to 9 and 10 days, respectively. The doubling time of FACS-sorted DsRed2⁺ cells remained 7 days. eGFP⁺ cells sorted at passage 8 could be propagated for eight population doublings in the presence of conditioned medium before ceasing to replicate, representing a 256-fold expansion. Growth arrest was not associated with detectable apoptosis, as judged by immunoblotting analysis for cleaved PARP (Fig. 7*C*). In contrast, p21, a protein involved in replicative senescence induced by telomere shortening (19), was upregulated in cells in the terminal passages (Fig. 7*C*). In contrast to

high-purity sorted eGFP⁺ cells, sorted eGFP⁺ cells with a purity <80% grew equally well in the presence or absence of conditioned medium, indicating that the residual non–β-cells remaining in those preparations were sufficient for conditioning the medium. eGFP⁺ cells sorted at passages 5–8 could be stained for Ki67 at multiple subsequent passages (Fig. 7*D*). Taken together, these results suggest that the eGFP⁻ cells secrete growth factor(s) needed for proliferation of eGFP⁺ cells and that the sorted eGFP⁺ cells become senescent around passage 16. This number of passages represents a theoretical overall expansion of 65,536-fold.

DISCUSSION

Our findings provide for the first time direct evidence for survival and dedifferentiation of cultured adult human β-cells. In addition, they demonstrate that the dedifferentiated cells can significantly proliferate in vitro. Dedifferentiation may be a precondition for β-cell proliferation in vitro, as evidenced by the scarcity of insulin⁺/Ki67⁺ cells

TABLE 1
Quantitative RT-PCR analysis of RNA from eGFP$^+$ and DsRed2$^+$ cells sorted at the indicated passages

Gene	eGFP$^+$		DsRed2$^+$		eGFP$^+$/DsRed2$^+$ at passage 2
	Passage 2	Passage 12	Passage 2	Passage 12	
Insulin	2.6688 ± 0.2894	0.0003 ± 8.33E-05	0.0634 ± 3.5E-03	ND	42.13
Glucokinase	3.9464 ± 1.5168	ND	0.0865 ± 0.0234	ND	46.29
PDX1	5.3896 ± 4.1185	ND	ND	ND	—
NEUROD1	10.2569 ± 0.6220	ND	2.2745 ± 0.1872	ND	4.52
NKX2.2	8.2412 ± 1.6133	ND	2.9353 ± 0.8095	ND	2.87
NKX6.1	6.9992 ± 0.6214	ND	0.8264 ± 0.1109	ND	8.56
HNF4α	4.8116 ± 0.5688	ND	0.6863 ± 0.2045	ND	7.29
PAX4	4.2179 ± 1.8572	ND	ND	ND	—
PAX6	20.1707 ± 2.5206	0.1231 ± 0.0126	4.0884 ± 0.3867	1.74E-03 ± 1.11E-03	4.94
PC1/3	7.4222 ± 0.3399	ND	0.0668 ± 0.0135	ND	112.20
PC2	5.3809 ± 0.4646	2.59E-04 ± 7.84E-05	2.1508 ± 0.1425	ND	2.50
GLUT2	13.7706 ± 2.8759	ND	ND	ND	—
Glucagon	5.6185 ± 2.2397	1.1E-03 ± 5.29E-04	9.1887 ± 3.7820	2.47E-03 ± 7.54E-04	0.61
Vimentin	154 ± 27	465 ± 193	181 ± 24	551 ± 111	0.84

Data are means ± SD ($n = 3$). Relative quantification normalized to human RPLP0 and expressed as percentage of the levels in unsorted islet cells at passage 0. ND, not detectable.

in early passages of human islet cell cultures (6). However, dedifferentiation may not be sufficient for inducing β-cell proliferation, as evidenced by the limited replication of dedifferentiated mouse β-cells. The ability to purify human β-cells after genetic labeling in vitro will allow detailed studies of the molecular mechanisms involved in these two processes. In addition to replicating cells derived from β-cells, the islet cell cultures contain replicating cells that are not labeled with eGFP. Some of these cells may also be derived from β-cells that were infected with only one or none of the two viruses. However, the majority of these cells are likely to be derived from other cellular origins, such as connective tissue in the islets or contaminating ductal tissue in the islet preparation. Nevertheless, our findings show that cells derived from β-cells can be isolated and expanded in the absence of other cell types present in the islet cell culture, provided that their culture medium is supplemented with medium conditioned by non–β-cells. The factors released by these cells that affect β-cell growth are of great interest, and the labeling system provides a convenient assay for their characterization. This system is also suitable for high-throughput screening of compound libraries for identification of agents that may further stimulate replication of the dedifferentiated β-cells in culture and induce redifferentiation of the expanded cells.

Our work demonstrates the feasibility of cell-specific labeling of cultured primary human cells using a genetic recombination approach that was previously restricted to transgenic animals. Despite the rapid dedifferentiation of β-cells in culture, virus integration into the genome and expression of the Cre recombinase under a β-cell–specific promoter are apparently fast enough to allow efficient DNA recombination before dedifferentiation occurs, resulting in a remarkable efficiency of β-cell labeling with this system (57.5 ± 8.9% of the C-peptide$^+$ cells after 5–6 days in culture). It should be noted that the cell specificity of this system relies on the use of a fragment of the regulatory region of the rat insulin II gene (-405 to $+7$ relative to the transcription start site), which is expected to allow Cre expression only in β-cells. However, although

this region was shown in numerous studies to contain the major regulatory elements required for β-cell–specific expression, it is possible that additional elements in the intact insulin gene locus are involved in determining tight cell specificity. Thus, it cannot be excluded that the absence of such elements in the RIP-Cre construct may result in its expression in a broader range of cells than bona fide mature β-cells.

Previous work has shown that proliferating cells expanded from cultured adult human islets contain cells expressing mesenchymal markers. Initially, it was suggested that these cells originated from β-cells through epithelial-to-mesenchymal transition (EMT) (7). Recent work has documented the expression of mesenchymal stem cell (MSC) markers on these cells, and their ability to differentiate into osteocytes and adipocytes (20,21); however, their cellular origin has not been rigorously established. Using the labeling system described here, it should be possible to determine whether these cells are generated from β-cells by EMT or represent MSCs originally present in the islets.

The proliferation of dedifferentiated human β-cells in culture is in contrast with the limited proliferative capacity of mouse β-cells cultured under the same conditions. It is possible that the culture media employed in this and previous (9–12) studies with mouse islet cell cultures lack components needed for a significant expansion of mouse β-cells, whereas they are supportive for human β-cell proliferation. Further investigation of this difference between mouse and human β-cells may provide new insights into the mechanisms that regulate β-cell replication.

for technical assistance; and Yuval Dor for comments on the manuscript.

REFERENCES

1. Dor Y, Brown J, Martinez OI, Melton DA: Adult pancreatic beta-cells are formed by self-duplication rather than stem-cell differentiation. *Nature* 429:41–46, 2004
2. Beattie GM, Itkin-Ansari P, Cirulli V, Leibowitz G, Lopez AD, Bossie S, Mally MI, Levine F, Hayek A: Sustained proliferation of PDX-1$^+$ cells derived from human islets. *Diabetes* 48:1013–1019, 1999
3. Beattie GM, Leibowitz G, Lopez AD, Levine F, Hayek A: Protection from cell death in cultured human fetal pancreatic cells. *Cell Transplant* 9:431–438, 2000
4. Halvorsen TL, Beattie GM, Lopez AD, Hayek A, Levine F: Accelerated telomere shortening and senescence in human pancreatic islet cells stimulated to divide in vitro. *J Endocrinol* 166:103–109, 2000
5. Beattie GM, Montgomery AM, Lopez AD, Hao E, Perez B, Just ML, Lakey JR, Hart ME, Hayek A: A novel approach to increase human islet cell mass while preserving β-cell function. *Diabetes* 51:3435–3439, 2002
6. Ouziel-Yahalom L, Zalzman M, Anker-Kitai L, Knoller S, Bar Y, Glandt M, Herold K, Efrat S: Expansion and redifferentiation of adult human pancreatic islet cells. *Biochem Biophys Res Commun* 341:291–298, 2006
7. Gershengorn MC, Hardikar AA, Wei C, Geras-Raaka E, Marcus-Samuels B, Raaka BM: Epithelial-to-mesenchymal transition generates proliferative human islet precursor cells. *Science* 306:2261–2264, 2004
8. Lechner A, Nolan AL, Blacken RA, Habener JF: Redifferentiation of insulin-secreting cells after in vitro expansion of adult human pancreatic islet tissue. *Biochem Biophys Res Commun* 327:581–588, 2005
9. Weinberg N, Ouziel-Yahalom L, Knoller S, Efrat S, Dor Y: Lineage tracing evidence for in vitro dedifferentiation but rare proliferation of mouse pancreatic β-cells. *Diabetes* 56:1299–1304, 2007
10. Chase LG, Ulloa-Montoya F, Kidder BL, Verfaillie CM: Islet-derived fibroblast-like cells are not derived via epithelial-mesenchymal transition from Pdx-1 or insulin-positive cells. *Diabetes* 56:3–7, 2007
11. Atouf F, Park CH, Pechhold K, Ta M, Choi Y, Lumelsky NL: No evidence for mouse pancreatic β-cell epithelial-mesenchymal transition in vitro. *Diabetes* 56:699–702, 2007
12. Morton RA, Geras-Raaka E, Wilson LM, Raaka BM, Gershengorn MC: Endocrine precursor cells from mouse islets are not generated by epithelial-to-mesenchymal transition of mature beta cells. *Mol Cell Endocrinol* 270:87–93, 2007
13. Castaing M, Guerci A, Mallet J, Czernichow P, Ravassard P, Scharfmann R: Efficient restricted gene expression in beta cells by lentivirus-mediated gene transfer into pancreatic stem/progenitor cells. *Diabetologia* 48:709–719, 2005
14. Thévenot E, Côté F, Colin P, He Y, Leblois H, Perricaudet M, Mallet J, Vodjdani G: Targeting conditional gene modification into the serotonin neurons of the dorsal raphe nucleus by viral delivery of the Cre recombinase. *Mol Cell Neurosci* 24:139–147, 2003
15. Cabrera O, Berman DM, Kenyon NS, Ricordi C, Berggren PO, Caicedo A: The unique cytoarchitecture of human pancreatic islets has implications for islet cell function. *Proc Natl Acad Sci U S A* 103:2334–2339, 2006
16. Leibowitz G, Oprescu AI, Uçkaya G, Gross DJ, Cerasi E, Kaiser N: Insulin does not mediate glucose stimulation of proinsulin biosynthesis. *Diabetes* 52:998–1003, 2003
17. Lukinius A, Ericsson JL, Grimelius L, Korsgren O: Ultrastructural studies of the ontogeny of fetal human and porcine endocrine pancreas, with special reference to colocalization of the four major islet hormones. *Dev Biol* 153:376–385, 1992
18. Bocian-Sobkowska J, Zabel M, Wozniak W, Surdyk-Zasada J: Polyhormonal aspect of the endocrine cells of the human fetal pancreas. *Histochem Cell Biol* 112:147–153, 1999
19. Zhang H: Molecular signaling and genetic pathways of senescence: its role in tumorigenesis and aging. *J Cell Physiol* 210:567–574, 2007
20. Davani B, Ikonomou L, Raaka BM, Geras-Raaka E, Morton RA, Marcus-Samuels B, Gershengorn MC: Human islet-derived precursor cells are mesenchymal stromal cells that differentiate and mature to hormone-expressing cells in vivo. *Stem Cells* 25:3215–3222, 2007
21. Gallo R, Gambelli F, Gava B, Sasdelli F, Tellone V, Masini M, Marchetti P, Dotta F, Sorrentino V: Generation and expansion of multipotent mesenchymal progenitor cells from cultured human pancreatic islets. *Cell Death Differ* 14:1860–1871, 2007